

## A low wind-noise microphone

von Hünenbein, Sabine<sup>1</sup>  
University of Salford  
M5 4WT Salford, Greater Manchester, UK

Bradley, Stuart<sup>2</sup>  
University of Auckland  
Private Bag 92019 Auckland, New Zealand

### ABSTRACT

Wind noise on microphones is problematic because of the possibility of overloading the microphone amplifiers and also because of potentially obscuring useful signals such as the low-frequency noise from wind turbines. While baffles certainly help, they may also modify the reception of signals of interest.

In response to this problem we describe a new approach where a closely-spaced array of microphones is mounted flush into a small-diameter surface. When wind is incident on this surface, a turbulent boundary layer forms (in fact the source of the wind noise on the microphones). However, the distance from individual microphones to the upstream leading edge of the surface varies depending on wind direction. The result is that the turbulent boundary layer properties are different for each microphone in the array. We use the properties of turbulent generated wind noise to determine the wind direction and the turbulent spectrum on the array. This allows for correction to mitigate the wind-generated noise.

**Keywords:** Aeroacoustic noise, Environment, Annoyance  
**I-INCE Classification of Subject Number:** 38

### 1. INTRODUCTION

Microphones record pressure fluctuations due to turbulence created in a boundary layer above the surface of the microphone [1]. These wind-dependent fluctuations can degrade the estimation of external sound. The output of the microphone is a time-varying voltage  $v_m$ . This voltage is the sum of:  $v_e$ , due to the external sound;  $v_w$ , due to the wind-generated noise; and  $v_n$ , due to microphone self-noise and preamplifier noise. The noise  $v_n$  can generally be neglected if the microphone and associated electronics are well designed so, in terms of spectral densities,

$$V_m = V_e + V_w. \quad (1)$$

---

<sup>1</sup> S.VonHunerbein@salford.ac.uk

<sup>2</sup> s.bradley@auckland.ac.nz

The aeroacoustic noise peaks at low audio frequencies and, in many applications, can be removed via spectral filtering. However, in applications such as recording the noise from wind turbines, the external signal of interest and the locally generated wind noise on the microphone have overlapping spectral peaks of comparable strength [2]. Directionality of microphones does not necessarily help. The usual approach is to use wind shields, but it may be necessary to have multiple, and physically large, shields. Alternative approaches, such as recording the external audio only during low-wind periods at the microphone, risk biasing data [3].

## 2. AEROACOUSTIC NOISE ON CLOSELY-SPACED MICROPHONES

### 2.1 The effect of boundary layer fetch

The spectral average of wind noise over one-third octave intervals at low frequencies depends on wind speed  $U$  and the distance  $d_m$  of the microphone from the upstream edge of the microphone casing [4]. If it is assumed that these dependencies are separable,

$$V_w = D_m W \quad (2)$$

where  $D_m$  is a function of boundary layer distance  $d_m$ , and  $W$  is a function of wind speed.

For  $M$  microphones, measurements  $V_{m,n}$ ,  $m = 1, 2, \dots, M$  are available in spectral intervals  $n = 1, 2, \dots, N$ . The sum of squares of residuals is

$$\chi^2 = \sum_{n=1}^N \sum_{m=1}^M [V_{e,n} + D_m W_n - V_{m,n}]^2 \quad (3)$$

Minimisation of  $\chi^2$  with respect to  $V_{e,n}$ ,  $W_n$ , and wind direction  $\phi$ , gives

$$\begin{aligned} V_{e,n} M + W_n \sum_m D_m &= \sum_m V_{m,n} \\ V_{e,n} \sum_m D_m + W_n \sum_m D_m^2 &= \sum_n \sum_m D_m V_{m,n} \\ \sum_m \dot{D}_m \sum_n V_{e,n} + \sum_n W_n \sum_m \dot{D}_m D_m &= \sum_n \sum_m \dot{D}_m V_{m,n} \end{aligned} \quad (4)$$

where  $\dot{D}_m = \frac{dD_m}{d\phi}$ . These equations can be rearranged to give

$$V_{e,n} = \frac{\sum D_m^2 \sum_m V_{m,n} - \sum D_m \sum_m D_m V_{m,n}}{\sum E_m} \quad (5)$$

$$W_n = \frac{M \sum_m D_m V_{m,n} - \sum D_m \sum_m V_{m,n}}{\sum E_m} \quad (6)$$

$$\sum_m [F_m(\phi) \sum_n V_{m,n}] = 0 \quad (6)$$

where

$$E_m = \sum D_m^2 - D_m \sum D_m$$

and

$$F_m = (E_m - \sum E_m) \sum \dot{D}_m + (M D_m - \sum D_m) \sum D_m \dot{D}_m \quad (7)$$

Equation 6 needs to be solved for wind direction  $\phi$  and hence  $D_m$  found. Then  $W_n$  is found from Equation 5, and the external sound spectral density  $V_{e,n}$  from Equation 4.

## 2.2 Distance and speed functions

In the configurations described below, the microphones are generally placed within a few millimetres of an edge and the relevant frequencies have wavelengths larger than about 100 mm. Ffowcs-Williams and Hall [5] show that, in this case, the mean square sound pressure generated by turbulent fluctuations on the microphones varies with frequency  $f$  and wind speed  $U$  as frequency  $(U/f)^5$ . In practice, wind tunnel studies on the microphone configuration discussed below find

$$V_w = \frac{a}{d_m^2} \frac{U^{5/2}}{1 + \left(\frac{f}{f_c}\right)^5} \quad (8)$$

where

$$f_c = b d_m^{1/4} U^{4/5}.$$

An example is shown in Figure 1.

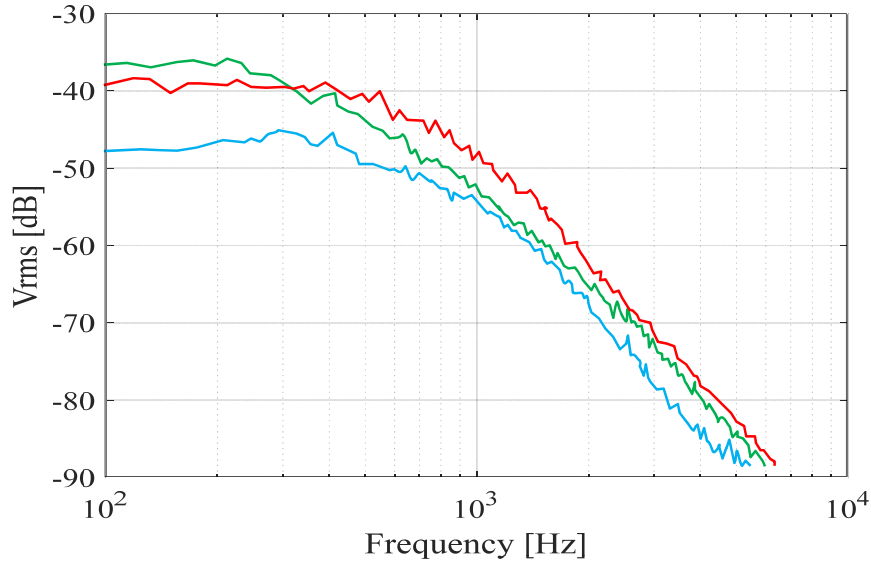


Figure 1. Wind tunnel results for  $U = 8 \text{ m s}^{-1}$ ,  $R = 34 \text{ mm}$ , and  $d = 10.5 \text{ mm}$  (green),  $15.5 \text{ mm}$  (red), and  $39 \text{ mm}$  (blue).

This means that, at low frequencies

$$D_m = \left(\frac{R}{d_m}\right)^2 \quad (9)$$

$$W_n = V_L \left(\frac{U}{U_0}\right)^{5/2}$$

and at high frequencies

$$D_m = \left(\frac{R}{d_m}\right)^{3/4} \quad (10)$$

$$W_n = V_H \left(\frac{U}{U_0}\right)^{13/2} \left(\frac{f_0}{f_n}\right)^5$$

where  $R$  is a reference length,  $V_L$  and  $V_H$  are constants depending on microphone type and amplifier,  $f_0$  is a reference frequency, and  $U_0$  is a reference wind speed.

### 2.3 Circular microphone arrays

The simplest configuration is two or more microphones each mounted at the centre of a circular disc, and with the disc radii,  $d_m$  in this case, being different for each disc. This configuration allows for easily solving for the 2 unknowns,  $V_e$  and  $U$ , and has the advantages of simplicity and independence of wind direction, but has the disadvantage of requiring several separated mountings.

A second configuration is a single disc with microphones mounted symmetrically around a circle. This circular array has the advantage of a single microphone casing. In this case the distances  $d_m$  depend on wind azimuth  $\phi$ , as shown in Figure 2.

The microphones are placed equally around a circle of radius  $r$  at angles

$$\phi_m = 2\pi \frac{m-1}{M} \quad m = 1, 2, \dots, M \quad (11)$$

and

$$d_m = R[p - \alpha \cos(\Delta\phi_m)] \quad (12)$$

where  $\alpha = r/R$ ,  $p = \sqrt{1 - \alpha^2 \sin^2(\Delta\phi_m)}$ , and  $\Delta\phi_m = \phi - \phi_m$ .

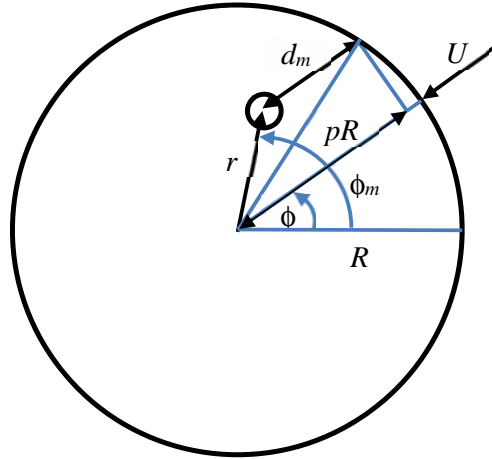


Figure 2. The geometry for multiple microphones placed on a circle of radius  $r$ .

This arrangement gives, for  $f_n \ll f_c$

$$D_m = \frac{1}{[p - \alpha \cos(\Delta\phi_m)]^2} \quad (13)$$

and

$$\dot{D}_m = -\frac{2\alpha \sin(\Delta\phi_m)}{p[p - \alpha \cos(\Delta\phi_m)]^2}. \quad (14)$$

### 3. SIMULATIONS FOR SPECIFIC DESIGNS

Three array arrangements were designed, all with  $R = 34$  mm, as shown in Figure 3 and defined in Table 1, with two versions of the  $M = 8$  array. The angle functions  $F_m$  are shown in Figure 4 for arrangement II.

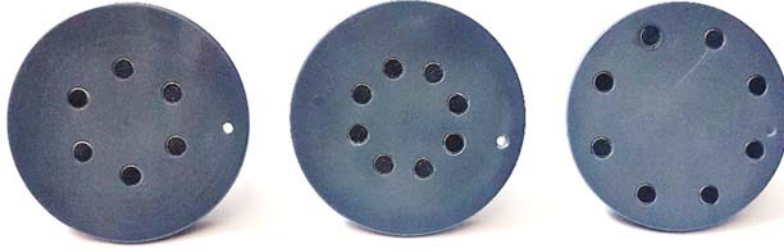


Figure 3. Array arrangements I (left), II (centre), and III (right).

Table 1. Dimensions of arrays.

Model	$M$	$r$ [mm]	$\alpha$
I	6	15	0.44
II	8	15	0.44
III	8	24	0.71

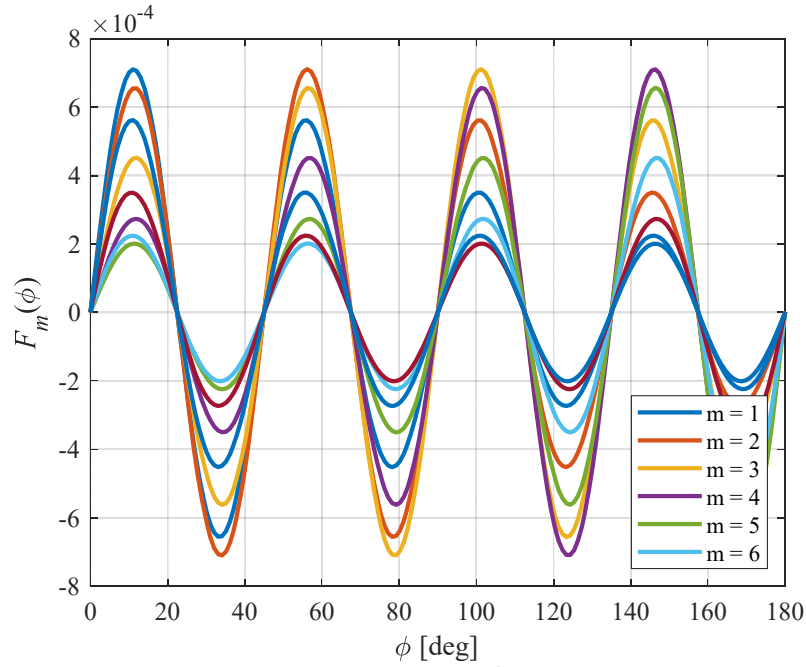


Figure 4 Angle functions  $F_m$  for arrangement II.

#### 4. FIELD VALIDATION

An initial investigation was set up as shown in Figure 5. Voltages from the eight microphones were recorded at a sampling rate of 40 kHz, together with the output from the sound level meter (which didn't have such a fast response, but it was simple to record its output at the same rate). Files were recorded and saved each 60 s. The Vaisala weather station has three ultrasonic time-of-flight paths which are used to estimate wind speed and direction. The wind output was averaged over the 60 s file duration. For the initial evaluation, around 8000 such files were recorded amounting to 250 Gb of data over 2 days. The winds were mostly light and variable, making analysis challenging. However, Figure 6 shows a typical 1/3-octave multiple spectrum for the array. The wind speed was  $1.5 \text{ m s}^{-1}$  from  $170^\circ$ , and there is, even at this low wind-speed, good separation between

the outputs from the 8 microphones. The dominant peak around 6 kHz is from cicadas, which were extremely loud at this time of the New Zealand summer and in a bush setting.



Figure 5. Preliminary field trial setup, showing SPL meter (left), Vaisala weather station (centre), and array arrangement III (right). Also shown at top right is the view of the array from slightly above.

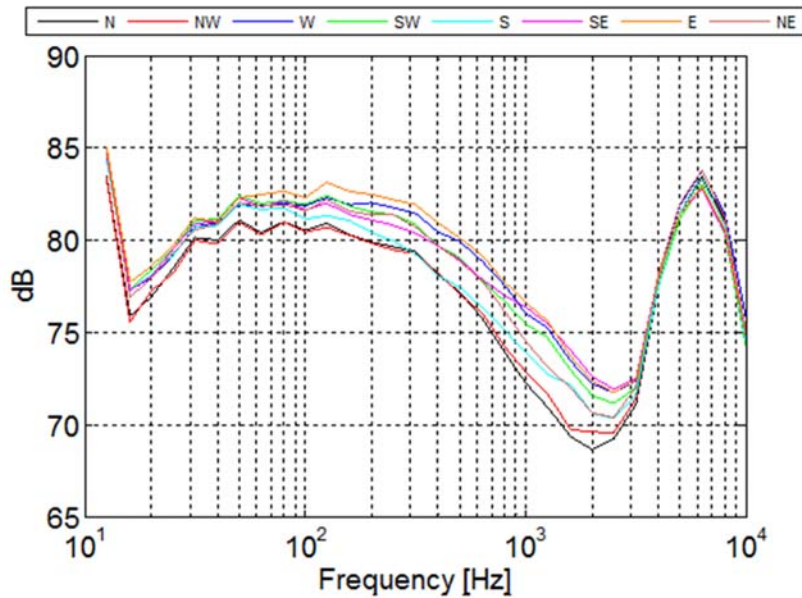


Figure 6. A typical one-minute 1/3 octave spectral output from the array. The wind speed was  $1.5 \text{ m s}^{-1}$  from  $170^\circ$ .

## 5. CONCLUSIONS

Wind noise on microphones arises from the turbulent boundary layer developed over the microphone surface. We describe a method which uses this boundary layer to identify the wind noise spectrum and to separate it from the spectrum due to a distant source of interest. The method relies on the established fact that the strength of the wind noise depends on the distance from the leading edge of the microphone mounting where the boundary layer is initiated. We show how the spectra can be separated into wind noise and external signal providing the dependence on downstream distance and the dependence on wind speed are separable. Wind tunnel tests on circular arrays shown that this is only true asymptotically at frequencies lower than or higher than a critical frequency. It is possible that two solutions can be found, one for each of these asymptotic limits, which would then provide a check on the wind noise retrieval.

Measurements have only so far been available in light wind conditions, but even at winds of less than  $2 \text{ m s}^{-1}$  separation between the spectra from the various microphones is apparent. This separation collapses as the wind speed goes to zero, as expected. These early observations are encouraging for further field studies and detailed analysis.

## 6. REFERENCES

1. Leo L. Beranek and István L. Vér, “*Noise and Vibration Control Engineering – Principles and Applications*”, edited by Leo L. Beranek and István L. Vér, John Wiley & Sons, New York (2006)
2. L. Cremer, M. Heckl, B.A.T. Petersson, “*Structure-Borne Sound - Structural Vibrations and Sound Radiation at Audio Frequencies*”, Springer (2005)
3. Sabine von Hünenbein, Paul Kendrick, and Trevor Cox, “*Extended simulations of wind noise contamination of amplitude modulation ratings*”, Wind Turbine Noise conference, 2 -5 May 2017, Rotterdam, NL, (2017)
4. Stuart Bradley, Tao Wu, Sabine von Hünenbein, and Juha Backman, “*The mechanisms creating wind noise in microphones*”, Audio Engineering Society Convention, Amsterdam, paper 5718, 9 pp, (2003).
5. J. E. Ffowcs-Williams and L.H. Hall “Aerodynamic sound generation by turbulent flow in the vicinity of a scattering half plane.” *J. Fluid Mech.* 40(4) pp. 657-670 (1970)